Fisheries and Environment Canada
Pêches et Environnement Canada

SCIENTIFIC SERIES NO. 78
(Résumé en français)

INLAND WATERS DIRECTORATE,
CANADA CENTRE FOR INLAND WATERS,
BURLINGTON, ONTARIO, 1977.

Fisheries and Environment Canada
Pêches et Environnement Canada

Development and Evaluation of an Experimental Frazil Ice Measurement Instrument

Gee Tsang

SCIENTIFIC SERIES NO. 78
(Résumé en français)

INLAND WATERS DIRECTORATE,
CANADA CENTRE FOR INLAND WATERS,
BURLINGTON, ONTARIO, 1977.

Cat. N° En: 36-502/78
ISBN 0-662-01551-7
CONTRACT NO. 08KX.KL229-7-1040
THORN PRESS LIMITED

Contents

Table

Illustrations

Illustrations (cont.)

Abstract

Theoretical investigations show that the presence of frazil ice in water can be quantitatively measured by its effect on the conductivity and the permittivity of the water. At frequencies much lower than 10^7 Hz, the frazil ice effect on conductivity predominates, and at frequencies much higher than 10^7 Hz, the ice effect on permittivity is predominant. An experimental instrument based on the resistance (i.e., conductivity) principle has been constructed and tested. Experiments were performed in a cold room with frazil ice produced in a beaker. The experiments showed that the laboratory instrument could quantitatively sense the presence of ice. The detailed circuit of the experimental instrument is shown. Some modifications of the circuit and the probe for improving the instrument are suggested as a consequence of the laboratory experiments and further theoretical investigations. The concentrations of frazil ice measured by the experimental instrument were by average about three times the concentration calculated theoretically. If the frazil ice crystals are assumed to have elongated spheroidal shapes with a length to breadth ratio of 10:1, the measured concentrations are about twice the calculated concentration. Further theoretical investigation is needed to explain this puzzle. The puzzle, however, is beneficial because it increases the sensitivity of the instrument.

This report describes phase I of an instrument development project. The design and production of an improved and manufacturable instrument will be phase II of the project.

Résumé

Des recherches théoriques démontrent que la présence du frazil dans l'eau est mesurable quantitativement par son effet sur la conductivité et la constante diélectrique de l'eau. Aux fréquences très inférieures à 10^7 Hz, c'est l'effet de conductivité du frazil qui prédomine tandis qu'aux fréquences très supérieures à 10^7, c'est celui de la constante diélectrique. Les chercheurs ont construit et essayé un appareil expérimental basé sur le principe de la résistance (p. ex. la conductivité). Des expériences en chambre froide ont produit du frazil dans un bécher et servi à démontrer que cet instrument de laboratoire pouvait mesurer la quantité de glace présente. Les détails des circuits de l'appareil expérimental sont illustrés. À la suite des expériences en laboratoire et des recherches théoriques subséquentes, certaines modifications du montage et de la sonde pourront être entreprises pour améliorer l'instrument. Les concentrations de frazil mesurées par l'appareil expérimental atteignaient en moyenne environ trois fois la concentration théorique calculée. Si les cristaux de frazil avaient la forme de sphéroïdes élongés espacés de dix fois leur longueur, les concentrations mesurées atteigneraient donc environ deux fois la concentration calculée. D'autres recherches théoriques sont nécessaires pour expliquer cette énigme; cependant, le problème est heureux puisqu'il accroît la sensibilité de l'appareil.

Le présent rapport décrit la phase I du projet de mise au point d'un appareil. La conception et la production d'un instrument amélioré et manufacturable constitueront la phase II du projet.

Development and Evaluation of an Experimental Frazil Ice Measurement Instrument

Gee Tsang

INTRODUCTION

Recently, noticeable progress has been made in many areas of ice research. Advances in frazil ice research, however, have remained limited because of, to a large extent, the lack of a working instrument which can quantitatively measure frazil ice.

Efforts have been made either in devising a technique to calculate the quantity of frazil ice or in developing an instrument to measure frazil ice concentration. Kristinsson (1970) measured the resistance between two wires wound spirally on an insulated rod immersed in frazil ice-laden water and correlated the resistance to the average frazil ice concentration over the depth of the rod. Gilfilian, Line and Osterkamp (1972) calculated the quantity of frazil ice formed in a river from the measured change in conductivity of the water, before and after ice formation. Kristinsson's instrument was crude and had been developed mainly empirically. The development was not under rigid theoretical guidance and lacked analytical refinement. No attempt was made by Gilfilian, Line and Osterkamp to create an instrument from their technique. The conceptual design of an instrument for sensing the frazil ice concentration, the velocity of the frazil ice and the velocity of the flowing water was proposed by Tsang (1974). The design is based on the same conductivity principle used by Kristinsson. Theoretical groundwork was laid to guide the design. An instrument based on laser principles was developed by Schmidt and Glover (1975). From the scattering of a laser beam by frazil ice crystals, the concentration of frazil ice and the velocity of the ice crystals were measured. The instrument could not be considered successful despite its complexity and high cost; it only gave accurate measurements at the early stage of ice formation and when the frazil ice concentration was low.

This report further develops Tsang's earlier concept of the instrument with respect to the frazil ice measurement component. The theoretical work is expanded to the effect of frazil ice on the impedance of the water, instead of on the conductance alone. Criteria are established to guide the design of a functional instrument for measuring frazil ice. An experimental instrument was constructed and its laboratory testing showed much promise. Refinement of the instrument, which is presently being undertaken, should produce a much needed instrument for fast and accurate frazil ice measurement at a low cost.

THEORY

Although pure water is electrically nonconductive, natural water is conductive because of mineral content. Natural water from different sources may have different conductivity because of varying mineral contents. In southern Ontario, the typical conductivity of natural water is of the order of 0.05 $(\Omega \cdot m)^{-1}$. As ice is formed from water impurities are rejected. Ice, therefore, may be considered nonconductive. From measuring the change of conductivity in water, the presence and quantity of frazil ice may thus be detected.

The dielectric constant of ice is also different from that of water. In addition, it is frequency-dependent. At low frequencies, the relative dielectric constant of ice is close to that of water, at about 80. As the frequency increases the dielectric constant of ice decreases. At 100 kHz, the relative dielectric constant of ice drops to about 5, whereas that of water remains the same at 80. Thus, the concentration of frazil ice in water may also be measured by sensing the change in the dielectric constant in water.

The immersion of two plates in water gives the equivalent electrical circuit of a resistance and a capacitance connected in parallel. The immersion of three plates in water, with the middle plate common to both side plates (Fig. 1), gives two such equivalent circuits. If ice is allowed to enter one pair of plates (probe x) and excluded from another pair of plates (probe y), the impedance given by the two probes will be different, even if the plates are the same size and the same distance apart. To measure the effect of frazil ice on the impedance of the ice-present sensor probe, as compared with the ice-free reference probe, an impedance bridge may be set up as shown in Figure 1. The fractional voltage drop across the two measuring points for the bridge is

$$\Delta = \frac{\Delta e}{e} = \frac{z_1}{z_1 + z_x} - \frac{z_2}{z_2 + z_y} \qquad (1)$$

where z is impedance and the subscripts indicate the four arms of the bridge.

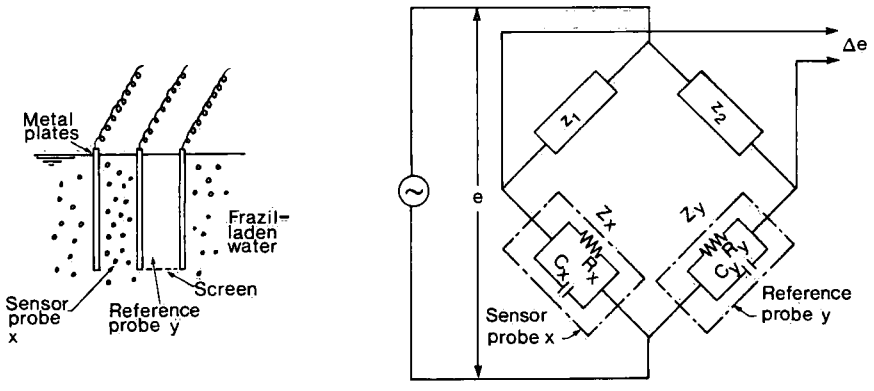

Figure 1. Equivalent circuit of three plates immersed in frazil-laden water and the bridge for measuring impedance changes.

Since z_y is not affected by the concentration of frazil ice c in the sensed volume of the sensor probe, and z_1 and z_2 can be made constant by design for a given frequency, the differentiation of equation (1) with respect to c is given by

$$\frac{d\Delta}{dc} = \frac{d}{dc} \left(\frac{z_1}{z_1 + z_x} \right) \tag{2}$$

Since z_x is a function of its resistance component, R_x, and reactance component, X_{cx}, and the latter are in turn functions of frazil ice concentration in the sensor probe, by chain differentiation rule, equation (2) becomes[1]

$$\frac{d\Delta}{dc} = - \frac{z_1}{(z_1 + z_x)^2} \left(\frac{\partial z_x}{\partial R_x} \frac{dR_x}{dc} + \frac{\partial z_x}{\partial X_{cx}} \frac{dX_{cx}}{dc} \right) \tag{3}$$

It is seen from Figure 1 that z_x is given by

$$z_x = \frac{R_x X_{cx}}{R_x + X_{cx}} \tag{4}$$

The application of equation (4) to equation (3) gives

$$\frac{d\Delta}{dc} = \frac{- z_1}{(z_1 + z_x)^2} \left[\left(\frac{X_{cx}}{X_{cx} + R_x} - \frac{R_x X_{cx}}{(X_{cx} + R_x)^2} \right) \frac{dR_x}{dc} + \left(\frac{R_x}{X_{cx} + R_x} - \frac{R_x X_{cx}}{(X_{cx} + R_x)^2} \right) \frac{dX_{cx}}{dc} \right] \tag{5}$$

To evaluate dR_x/dc and dX_{cx}/dc in equation (5), the functional form of R_x and X_{cx} must be known. The resistance between the two plates of the reference probe is[2]

$$R_y = \frac{\rho_0 S}{A} \tag{6}$$

where ρ_0 is the resistivity of the ice-free water and A and S are the plate surface area and the separation between the plates, respectively. For the sensor probe, the presence of frazil ice reduces the conductive volume and hence increases the resistivity of the

[1]For clarity of mathematical expression, the imaginary number indicator j associated with reactance is absorbed into X_{cx} and other similar reactance notations in this report.

[2]Strictly speaking, equation (6) is only correct when the two plates are very close together and the stray effect is negligible. For plates of some distance apart, a corrective coefficient has to be introduced. This coefficient is not shown here because it will be cancelled out subsequently and will not affect the final theoretical outcome.

medium between the plates. If the frazil ice is assumed to be finely and uniformly suspended in the water, the increase in resistivity will be proportional to the volumetric presence of frazil ice in the water, and one may write

$$R_x = \frac{\rho_0}{(1 - c)} \frac{S}{A} \tag{7}$$

From equations (6) and (7), one has

$$\frac{R_x}{R_y} = \frac{1}{(1 - c)} \tag{8}$$

and its differentiation with respect to c gives

$$\frac{dR_x}{dc} = \frac{R_y}{(1 - c)^2} \tag{9}$$

The capacitance formed by the two plates of the reference probe is given by[3]

$$C_y = \varepsilon_{H_2O} \frac{A}{S} \tag{10}$$

where ε_{H_2O} is the absolute dielectric constant of water. For the sensor probe, because of the presence of frazil ice, the dielectric constant ε_x will be different from ε_{H_2O}. Intuitionally speaking, ε_x should be a function of ε_{H_2O}, the dielectric constant of ice ε_{ice}, the concentration of frazil ice in the sensor probe and some other secondary factors. Since the exact functional relationship is not known, one may assume a simple proportional law of

$$\varepsilon_x = (1 - c) \varepsilon_{H_2O} + c \varepsilon_{ice} \tag{11}$$

The capacitance formed by the two plates of probe x, therefore, is given by

$$C_x = \left[(1 - c) \varepsilon_{H_2O} + c \varepsilon_{ice}\right] \frac{A}{S} \tag{12}$$

The reactances produced by C_x and C_y are, respectively,

$$X_{cx} = - \frac{j}{2\pi f C_x} \quad \text{and} \quad X_{cy} = - \frac{j}{2\pi f C_y} \tag{13}$$

[3]See Footnote 2.

where $j = \sqrt{-1}$ and f is the frequency of the applied voltage. From equations (10), (12) and (13) one obtains

$$\frac{X_{cx}}{X_{cy}} = \frac{C_y}{C_x} = \frac{1}{1 - c + c\gamma_\varepsilon} \tag{14}$$

where $$\gamma_\varepsilon = \frac{\varepsilon_{ice}}{\varepsilon_{H_2O}} = \text{ratio of dielectric constants} \tag{15}$$

The differentiation of equation (14) with respect to c gives

$$\frac{dX_{cx}}{dc} = \frac{1 - \gamma_\varepsilon}{(1 - c + \gamma_\varepsilon c)^2} X_{cy} \tag{16}$$

The substitution of equations (9) and (16) into equation (5) and then the expression of z_x, R_x and X_{cx} by equations (4), (8) and (14) will produce a rather complicated function of $d\Delta/dc$ in the form of

$$\frac{d\Delta}{dc} = f\left(z_1, c, X_{cy}, R_y, \gamma_\varepsilon\right) \tag{17}$$

and its integration will give the relationship between the signal output Δ and frazil ice concentration. Although the mathematical operations for obtaining the final relationship are numerically possible, it is not advisable for an instrument to be based on such a complicated mathematical relationship. The relationship can be greatly simplified by imposing some constraints on the bridge circuit.

It is seen from equation (4) that if X_{cx} is very much larger than R_x, z_x will be approximately equal to R_x. Conversely, if R_x is very much greater than X_{cx}, z_x will approach X_{cx}. For the former case, from

$$\left|\frac{-j}{2\pi f C_x}\right| \gg R_x \tag{18}$$

and equations (8) and (14), one has

$$\frac{1 - c + c\gamma_\varepsilon}{2\pi f C_y} \gg \frac{R_y}{1 - c} \tag{19}$$

The substitution of equations (6) and (10) into equation (19) gives

$$f \ll \frac{1 - c + c\,\gamma_\varepsilon}{2\pi\,\varepsilon_{H_2O}\,\rho_0} \tag{20}$$

Since the largest value of γ_ε can only be about unity and under both laboratory and field conditions, frazil ice concentration seldom exceeds a few percent. The terms containing c in equation (20) may be dropped without seriously affecting the equation. The resistivity of the ice-free water in the reference probe ρ_0 is not a constant; it decreases continuously as ice is formed and impurities are rejected into the water. If the conducting capability of water is considered to be proportional to the number of ions in the water, one may write

$$\rho_0 = (1 - \bar{c})\ \rho_{H_2O} \tag{21}$$

where ρ_{H_2O} is the resistivity of the water at 0°C, but before the production of ice, and $\bar{c}$ is the mean frazil ice concentration in the water. Since $\bar{c}$ is of the same order of magnitude as c, it may be dropped from equation (21) thus giving $\rho_0 \simeq \rho_{H_2O}$. With respect to the discussions above, equation (20) is reduced to

$$f \ll \frac{1}{2\pi\ \varepsilon_{H_2O}\,\rho_{H_2O}} \tag{22}$$

The value of the absolute dielectric constant of water is approximately

$$\varepsilon_{H_2O} = 80\ \varepsilon_{vacuum}$$
$$= 80 \times \frac{1}{36\pi} \times 10^{-9} \quad \text{farads per metre}$$

and the typical value of ρ_{H_2O} of natural water is

$$\rho_{H_2O} = 20 \quad \text{ohm metres}$$

The substitution of the values above into equation (22) gives

$$f \ll 10^7 \quad \text{hertz} \tag{23}$$

When the condition above is satisfied, the reactance X_{cx} may be disregarded and one has

$$z_x = R_x \tag{24}$$

On the other hand, if

$$f \gg 10^7 \text{ hertz} \tag{25}$$

then the resistance R_x from equation (4) may be disregarded and one has

$$z_x = X_{cx} \tag{26}$$

The frequency of 10^7 Hz is in the HF (high frequency) range or the decametric wave range. There is no technical difficulty in the present technology both in furnishing equations (23) and (25) and in handling the signals. Thus, by choosing an appropriate frequency, the bridge can be made either resistance- or reactance-predominant.

When equation (23) is satisfied, equation (5) is reduced to

$$\frac{d\Delta}{dc} = \frac{-z_1}{(z_1 + R_x)^2} \frac{dR_x}{dc} \tag{27}$$

The substitution of equations (8) and (9) into equation (27) and the assignment of z_1 to consist of resistance R_1 alone give

$$\frac{d\Delta}{dc} = \frac{-R_y/R_1}{(1 - c + R_y/R_1)^2} \tag{28}$$

Since c is small compared with unity, it may be dropped from the right-hand side of equation (28) without seriously affecting the outcome. Thus, one has

$$\frac{d\Delta}{dc} = \frac{-R_y/R_1}{(1 + R_y/R_1)^2} \tag{29}$$

The resistance between the two plates of probe y at 0°C, but before the production of ice in the water, is given by

$$R_{y_0} = \rho_{H_2O} \frac{S}{A} \tag{30}$$

From equation (30) and equations (6) and (21), one sees

$$R_y = (1 - \bar{c}) R_{y_0} \tag{31}$$

The substitution of equation (31) into equation (29) and the writing of

$$\frac{R_{y_0}}{R_1} = N \tag{32}$$

give $$\frac{d\Delta}{dc} = \frac{(\bar{c} - 1)\, N}{[1 + (1 - \bar{c})\, N]^2} \tag{33}$$

and the integration of the equation above gives

$$\Delta = \frac{(\bar{c} - 1)\, N}{(1 + N - \bar{c}\, N)^2}\, c \tag{34}$$

which is a linear relationship. Equation (34) is integrated under the boundary condition that $\Delta = 0$, when $c = 0$. This boundary condition requires the bridge to be balanced at zero ice presence in the sensor probe.

Equation (34) is not strictly a linear relationship because the proportional coefficient is a function of $\bar{c}$ which changes as frazil ice is continuously formed. Therefore, except for instantaneous measurement, such as for obtaining the concentration profile along a vertical at a given instance, the signal output and frazil ice concentration in probe x are not linearly proportional. Since $\bar{c}$ is small compared with unity, the effect of $\bar{c}$ on the constancy of the proportional coefficient of equation (34) should not be great.

Equation (34) shows that the signal output from the bridge depends on the resistance ratio N. Since the conductivity of natural water varies over a wide range from place to place, N depends on the source of water for a constant R_1 on the bridge. From the above, one sees that the signal-frazil ice concentration relationship may not be calibrated from one sample of water for other samples of water. For practical use of the instrument, the bridge should be designed in such a way as to give a constant N for water of different conductivity. This can be easily done electrically, as will be discussed later.

When high frequencies satisfying equation (25) are used, equation (5) is reduced to

$$\frac{d\Delta}{dc} = \frac{-z_1}{(z_1 + X_{cx})^2}\, \frac{dX_{cx}}{dc} \tag{35}$$

The substitution of equations (14) and (16) into equation (35) and the assignment of z_1 to consist of reactance X_{c_1} alone give

$$\frac{d\Delta}{dc} = \frac{-(1 - \gamma_\varepsilon)\, X_{cy}/X_{c_1}}{(1 - c + \gamma_\varepsilon c + X_{cy}/X_{c_1})^2} \tag{36}$$

Denoting

$$M = \frac{X_{cy}}{X_{c_1}} = \frac{C_1}{C_y} \tag{37}$$

where C_1 is the capacitance producing X_{c_1} and dropping the terms containing c on the right-hand side of equation (36) because of their relatively small magnitude result in

$$\frac{d\Delta}{dc} = \frac{(\gamma_\varepsilon - 1)\, M}{(1 - M)^2} \tag{38}$$

The integration of the previous equation gives

$$\Delta = \frac{(\gamma_\varepsilon - 1)\, M}{(1 - M)^2}\, c \tag{39}$$

a linear relationship similar to equation (34). The boundary condition leading to equation (39) also requires the bridge to be balanced at zero frazil ice concentration in the sensor probe.

Comparing equations (34) and (39), one sees that although the former is sensitive to $\overline{c}$, the latter is not affected by the production of ice. Also, while N in equation (34) is affected by the conductivity of water for a given R_1, M in equation (39) is not affected by the source of water. Thus, if the technical difficulty of employing a capacitance bridge and a resistance bridge is about the same and the costs are comparable, capacitance sensing of frazil ice is preferable because equation (39) is a "truer" linear equation than equation (34) and one need not be concerned about the change of M, from one source of water to another.

INSTRUMENT DEVELOPMENT

The development work reported herein is aimed to verify the theoretical principles mentioned in the last section and is defined as phase I of the development. Further refinement of the theory and the production of a manufacturable prototype instrument will make up phase II of the development. During phase I, the first intention was to develop an experimental instrument based on the capacitance sensing principle. Such a plan had to be postponed because the company under contract for the design and construction of the hardware did not have a HF generator and there were some trivial technical problems. The plan was changed to the development of an experimental instrument based on the resistance sensing principle and its testing.

The Probe

Figure 2 shows the experimental probe. It consists of three stainless steel plates, 1 cm wide by 2 cm long and separated by 1 cm. Each plate was soldered onto two brass stems, 1 mm in diameter. The stems were 1.5 cm long, with fine, insulated resistance wire wound around them as heaters. The coils on the two stems of each plate were connected in series, but the heaters for the three plates were connected in parallel. Each heater coil had a resistance of approximately 8 Ω. The stems and heaters were imbedded together in plastic insulation (Scotch cast) to prevent short circuits resulting from abrasion and burning out of the heaters' protective coatings. Between one pair of plates (probe x) the space at the sides was left open, and between the second pair of plates (probe y) the space at the sides was sealed by Teflon plates a little less than 1 mm thick. Small holes, 1 mm in diameter, were drilled in two side Teflon plates through which water could pass into and out of the probe to give a representative sample of the water to the reference probe. The bottom Teflon plate was not perforated so that the ice formed in the ambient water could not float into the sensed volume. Also little ice could enter the reference probe from the side because the perforated holes were perpendicular to the vertical direction of ice movement.

Ideally, the sensor probe and the reference probe should be identical and have the same resistance (and capacitance). This was impossible because (1) the probes were hand-made and (2) although Teflon plates were used as spacers between one pair of probe plates, they were absent between the second pair. The probes were also structurally not very rigid; accidental banging and twisting during their employment and cleansing could easily change the resistance and capacitance. A protective cap made of a short section of Plexiglas tubing with large holes drilled on the side and a nylon screen glued to the bottom was later used to protect the probes. The cylindrical body above the probes housed the electrical joints and provided a structural base for the probes (Fig. 2). It was too large for these purposes and could be greatly reduced in size or eliminated altogether.

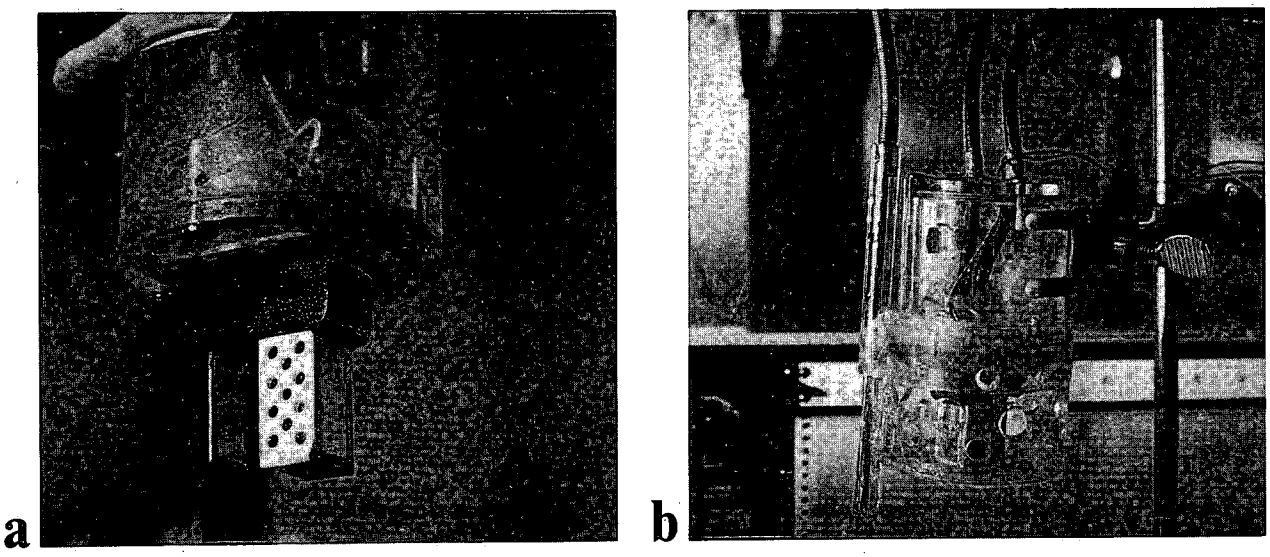

Figure 2. (a) The experimental probe and (b) probe with protective cap and thermistor.

The heaters were for preventing the nucleation of ice on the probe plates, the adhesion of ice to the plates of the sensor probe and the formation of ice in the reference probe. If the rate of cooling of water is dT/dt, from supplying a heat flux by the heaters to compensate such a rate of cooling, one has

$$P = \frac{2 \times 4.186\ V}{\eta} \frac{dT}{dt} \tag{40}$$

for the reference probe, where P is the power to the reference probe's heaters in watts, V is the volume of the reference probe in cubic centimetres, dT/dt is in °C/s, η is the efficiency of heat transmitted from the heaters to the probes, 4.186 is a conversion factor and 2 is introduced because only half of the heat is going to the sensed volume. Equation (40) tends to be conservative because due to the slow motion of the water in the caged reference probe, the rate of heat loss should be less than that of the ambient water. From equation (40), the voltage of the dc source applied to the reference probe's heaters is given by

$$v = 2.89 \sqrt{\frac{RV}{\eta} \frac{dT}{dt}} \quad \text{volts} \tag{41}$$

where R is the resistance of the reference probe's heaters in ohms. For the constructed experimental probe, since the heaters were imbedded in insulation, a heating efficiency of $\eta \doteq 1.00$ was assumed. For the sensor probe (actually the side plate that forms the sensor probe), less heat is needed. Ideally, a feedback system should be built into the heaters so that the plates of the sensor heater are maintained at a temperature slightly above freezing. For the experimental probe, however, because of easy construction, the heaters for the sensor probe were made in the same way as the reference probe's heater and had the same heat input. It was reasoned that since frazil ice is formed under turbulent conditions, the heat dissipated into the water in the unconfined sensor probe is likely to have diffused into the ambient water in a short time, instead of accumulating sufficiently around the probe to affect the reading. In mathematical terms, one may say that since the convective variation of frazil ice concentration in the sensor probe very much outweighs the temporal variation which is affected by local heat input, the effect of local heat input on the total variation of frazil ice concentration may be overlooked.

This reasoning is acceptable prior to ice formation, during the period of ice formation and when the concentration of frazil ice is low. When the concentration of frazil ice is high, the turbulence in the water is greatly suppressed and the movement of ice in the water is greatly reduced. In such a situation, a high rate of heat input will lead to fast melting of the ice and an erroneous reading. If the frazil ice is assumed to stay in the sensor probe, then from the rate of heat flux and the consequent melting of ice one obtains

$$P = \frac{616\ V\ c}{\eta} \left(\frac{dc/dt}{c}\right) \text{ watts} \qquad (42)$$

where $(dc/dt)/c$ is the relative time rate of frazil ice concentration reduction in s^{-1} and its reciprocal gives the time in seconds for all the ice to melt. For the experimental probe, equation (40) was used to regulate the heaters prior to, and during, frazil ice formation, and equation (42) was used after frazil ice was formed in the experiments.

For good heat conduction from the heater to the probe plates, the heating coils have to be tightly wound against the plate stems; this introduces electronic implications because high capacitance is formed between the heating coils and the probe stem. If the heaters are connected to a common power source, as in the case of the experimental probe, then, in addition to the capacitance formed between two probe plates, there are two capacitances formed by the coils and the stems and connected in series for each probe, as shown in Figure 3. For the experimental probe, the additional high capacitance made the sensing bridge an impedance bridge instead of a resistance bridge. Before the heaters were imbedded in the plastic insulation, the seeping of water into the space between the coils and the stems had frequently upset the balance of the bridge. The presence of the additional capacitances had been overlooked and it took some time before their discovery.

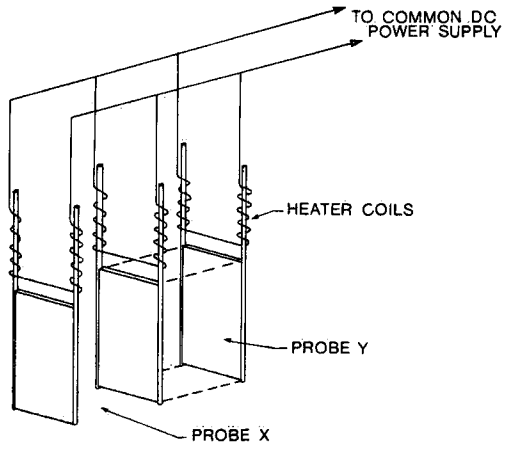

a

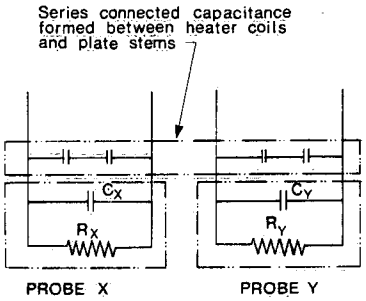

b

Figure 3. Capacitance introduced by heaters: (a) heater arrangement of experimental probe and (b) equivalent circuit of probe with heaters.

Since the capacitance between the heating coils and the probe stems can be quite high in comparison with the capacitance between two probe plates, it can completely mask the latter and render an instrument built on the capacitance sensing principle inoperative. To minimize the effect of this unwanted large capacitance for an instrument built on the resistance sensing principle, one may lower the frequency of the ac voltage applied to the bridge. For an instrument built on the capacitance sensing principle, the corrective measures are more difficult and require more thinking. A simple way to eliminate this additional capacitance is to have independent power supplies to the heaters of each probe plate. Yet this requires cumbersome power sources and is unsound with respect to technical and engineering aspects.

The outer surface of the side plates of the probes should be insulated so that the sensed volume is confined within the probes. For the experimental probe, however, this was not done because the contractor could not find suitable insulating material that would cling tightly to stainless steel. Since the construction of the experimental probe confined most of the electric line to the space between the plates, the stray effect caused by the exposed outer plate surfaces was overlooked.

The Circuitry

Derived from earlier theoretical investigations, the essential components of a basic instrument based on resistance sensing are shown in the block diagram in Figure 4. In the diagram, the signal of frazil ice concentration is picked up by the bridge. In the bridge, resistances R_{xp} and R_{yp} and capacitances C_{xp} and C_{yp} are connected parallel to probe x and probe y. They are for fine resistance and capacitance adjustments of the probes because the two probes cannot be made identical. If the frequency of the applied voltage is sufficiently low, C_{xp} and C_{yp} may be disregarded altogether. The LF voltage is provided by the LF generator in Figure 4. Apparently, the frequency cannot be too low, otherwise polarization will occur. The bridge output is fed into an amplifier by way of a transformer. The amplified signal, after being rectified, is shown on the signal display.

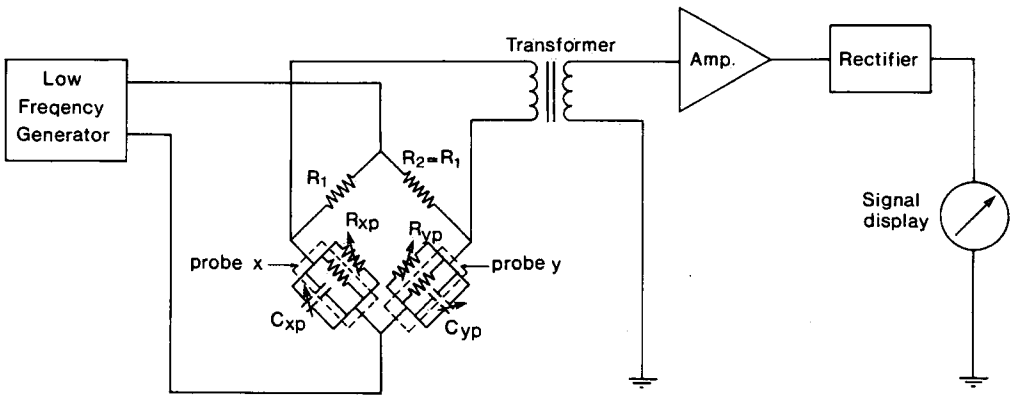

Figure 4. Block diagram for frazil instrument, based on resistance sensing.

The diagram in Figure 4 can be advanced to that shown in Figure 5. In Figure 5, the amplitude of the LF ac generator is made variable by means of potentiometer R_A. The fine adjustment of resistance equilibrium of the bridge is also obtained by the use of a potentiometer (variable resistance) and the fine adjustment of capacitance equilibrium is provided by the use of a fixed capacitance C_{xp} and a variable capacitance C_{yp}. The range of C_{yp} to be twice the magnitude of C_{xp} means that C_{yp} can be adjusted to less than or greater than C_{xp} as much as the magnitude of C_{xp}. Switch S_1 can be connected to one of the terminals a, b, c or d. Because the resistances R_a, R_b, R_c and R_d are progressively one less than the other in that order, for the same voltage output after the rectifier, the current through the resistances will be progressively larger.

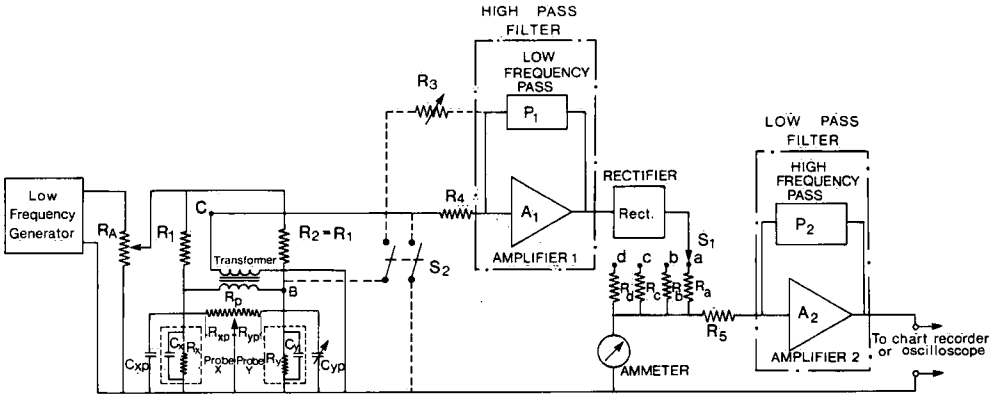

Figure 5. Basic design of frazil ice instrument.

The calibration of the signal display, or the ammeter deflection, can be made by connecting two known resistances R_x and R_y to the probe connectors with R_x, e.g., 1% greater than R_y. The bridge will then become unbalanced and the unbalanced signal is shown by the ammeter. The deflection of the ammeter can be made to reach the full range of the meter by adjusting the amplitude of the ac voltage input to the bridge through R_A. The replacement of R_x and R_y by the sensor and the reference probes then will enable the instrument to sense frazil ice concentration theoretically from 0 to 1%.

If, for example, the calibration above is done for switch S_1 at position d and the ratio of the resistances is $R_a:R_b:R_c:R_d = 10:5:2:1$, a full-range deflection of the ammeter when S_1 is at d will only give ammeter deflections of 0.5, 0.2 and 0.1 of the full range, respectively, when switch S_1 is switched to positions c, b and a. In other words, four different sensitivity ranges of 0-1%, 0-2%, 0-5% and 0-10% can be obtained by simple switching of S_1 to the four different positions. Although four sensitivity ranges, as shown above, were used for the experimental instrument, there is no restriction on the number and sensitivity of the ranges. This discussion is only quantitatively valid when the internal resistance of the signal output system is small compared with resistances R_a to R_d.

In describing the calibration procedure above, it was only required that R_x be 1% greater than R_y and the absolute value of R_y not be specified. It is seen from the earlier theoretical investigations [equation (29)] that the full deflection of the ammeter is also affected by the absolute value of R_y. Thus, for different R_y's, R_A has to be adjusted each time. The difference in the conductivity of water from varying sources means that R_y will change from one water sample to another or the instrument will have to be calibrated each time using an electrical resistor having exactly the same resistance as that between the two probe plates when immersed in the particular water. To overcome this problem, a calibration switch S_2 and a variable resistance R_3 shown by dashed lines in Figure 5 were used in the experimental instrument. When S_2 is open, the calibration described earlier is not affected by the presence of R_3 and a full-range deflection of the ammeter can be obtained by adjusting R_A as if R_3 were not there. After the full-range deflection is obtained, the voltage at point C and the voltage at point B will have a one-to-one correspondence relationship. When S_2 is closed, the input to amplifier 1 will be the voltage at B, by way of R_3, instead of the voltage at C, by way of the constant resistor R_4. Now R_3 may be adjusted to give a full-range deflection of the ammeter. After fixing this R_3 setting, any R_A setting that gives a full deflection of the ammeter by way of C will also give a full deflection of the ammeter by way of B. With the conclusion above, for different values of R_y because of different sources of water one may close switch S_2 and adjust R_A for a full ammeter deflection. Once this is obtained, the opening of S_2 and the placement of R_y and $R_x = 1.01\ R_y$ will also give a full ammeter deflection.

This arrangement is only valid if the functional relationship between the potential at C and the potential at B is independent of the value of R_y, or rather the ratio of R_2/R_y. This, however, is not the case because the earlier theoretical investigations show that the potential at C, which is actually the bridge signal output, is a function of both R_x/R_y and R_2/R_y. On the other hand, since point B is on the arm of the bridge containing R_2 and R_y, the potential at point B should also be affected by R_2/R_y. Thus, the functional relationship between the potential at C and the potential at B depends on R_2/R_y, and the calibration is physically unsound. This physical drawback was not perceived when designing the instrument. Because water from the same tap was used for the evaluation tests, R_3 and S_2 were not eliminated from the experimental instrument after the drawback was found. The small daily variation of the resistivity of the water probably would only have a negligible effect on the initial calibration, and the incorporation of R_3 and S_2 in the instrument would make daily operation much easier. For the final version of the instrument, this part of the circuitry had to be eliminated and replaced by a more appropriate circuit shown later in this report.

For showing the signals on an oscilloscope and for recording the signals on a chart or tape recorder, the signal input to the ammeter is further amplified by amplifier 2, as shown in Figure 5.

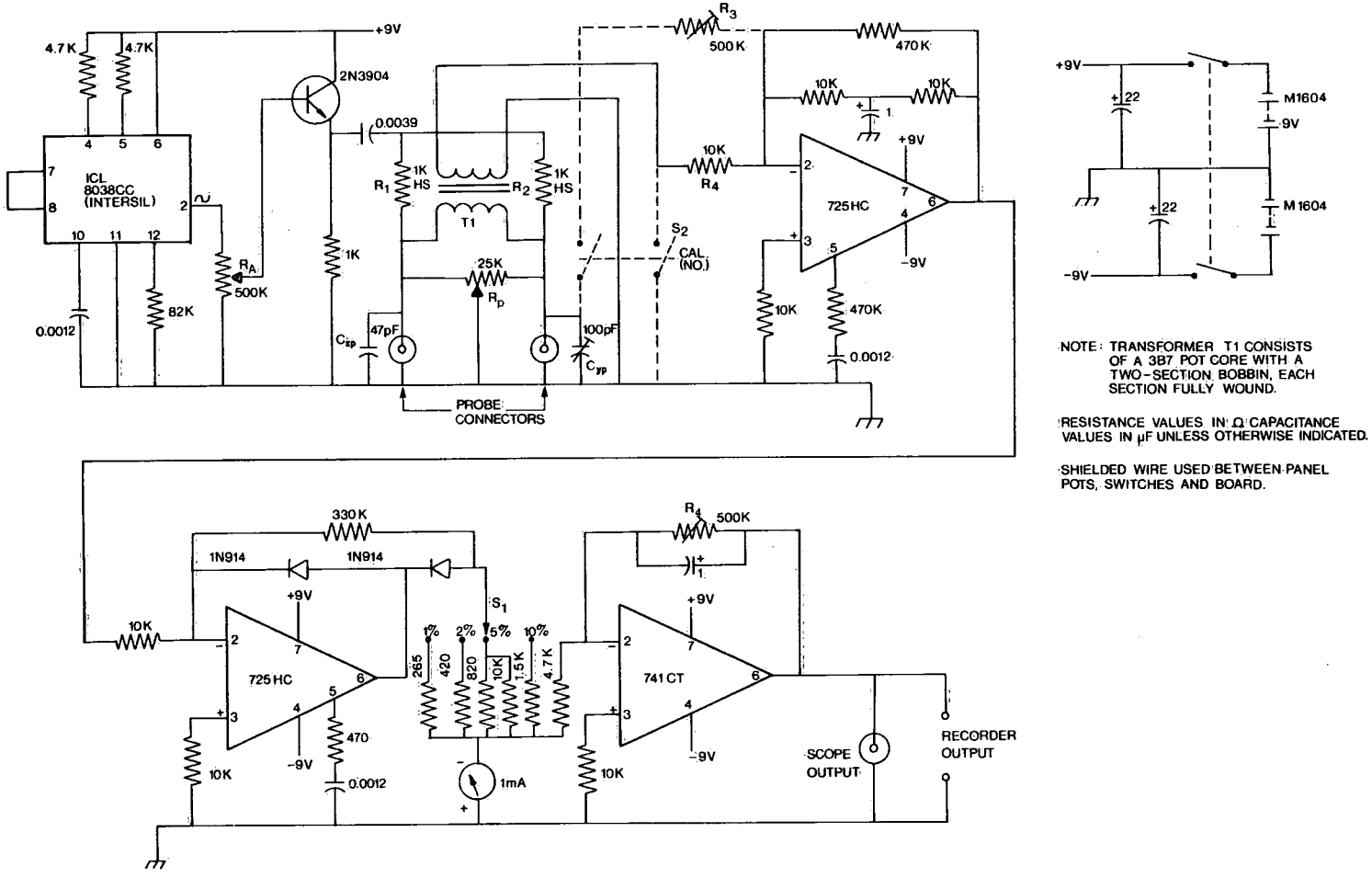

NOTE: TRANSFORMER T1 CONSISTS OF A 3B7 POT CORE WITH A TWO-SECTION BOBBIN, EACH SECTION FULLY WOUND.

RESISTANCE VALUES IN Ω CAPACITANCE VALUES IN μF UNLESS OTHERWISE INDICATED.

SHIELDED WIRE USED BETWEEN PANEL POTS, SWITCHES AND BOARD.

Figure 6. Electronic circuit of experimental instrument for frazil ice sensing.

The detailed design of the experimental instrument is shown by the circuit diagram in Figure 6. A 50-kHz ac generator was used for the bridge (Fig. 6). This frequency is sufficiently low compared with the critical frequency of 10^7 Hz. The power supply to the heater is not indicated in the diagram. The ratios of $R_a:R_b:R_c:R_d$ are not exactly 10:5:2:1. Figure 7 shows the experimental instrument and its connection to the experimental probe.

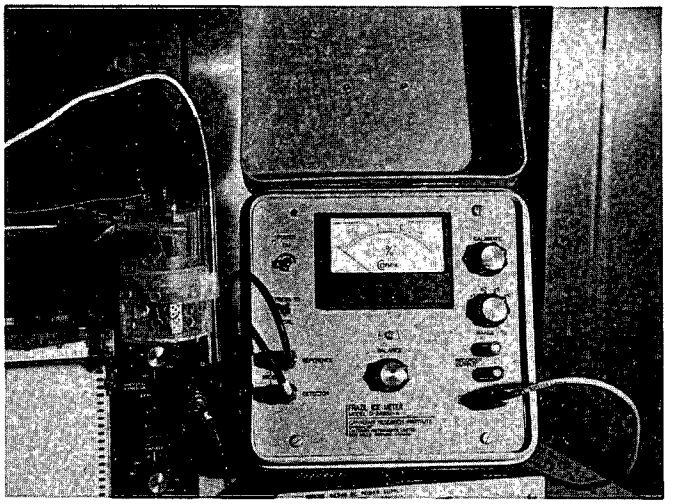

Figure 7. Experimental instrument and its connection to the probe.

TESTING AND EVALUATION OF THE EXPERIMENTAL INSTRUMENT

The experimental instrument was tested in a cold room. The experimental setup is shown on Figure 8. The experimental probe was immersed in a 1000-ml beaker on top of a magnetic stirrer (Fig. 8). The turbulence in the beaker was generated by the swirl of a magnetic bar. The probe was placed so that the Scotch cast base was just in the water. The protective cap was put over the probe. The placement was carefully adjusted so that the screen at the end of the cap was very close to the end of the probe plates. Therefore, the frazil ice in the probe was generated in the water inside the cap over the probe's depth. The beaker was placed in front of a two-speed fan. By adjusting the stirrer and fan speeds, and the distance between the beaker and the fan, different cooling rates could be obtained. The stirrer and especially the fan greatly affected the cooling rate of the water. When both the fan and the stirrer were off, the cooling rate was reduced by one or two orders of magnitude. A thermistor-type thermometer calibrated and accurate to 0.01°C was secured to the protective cap. The temperature output was recorded by a chart recorder as well as displayed on a digital voltmeter outside the cold room. The signal output from the probe was also chart-recorded. A dc power supply provided the power to the heaters of the probe. For all the experiments, the cold room was maintained at about -10°C.

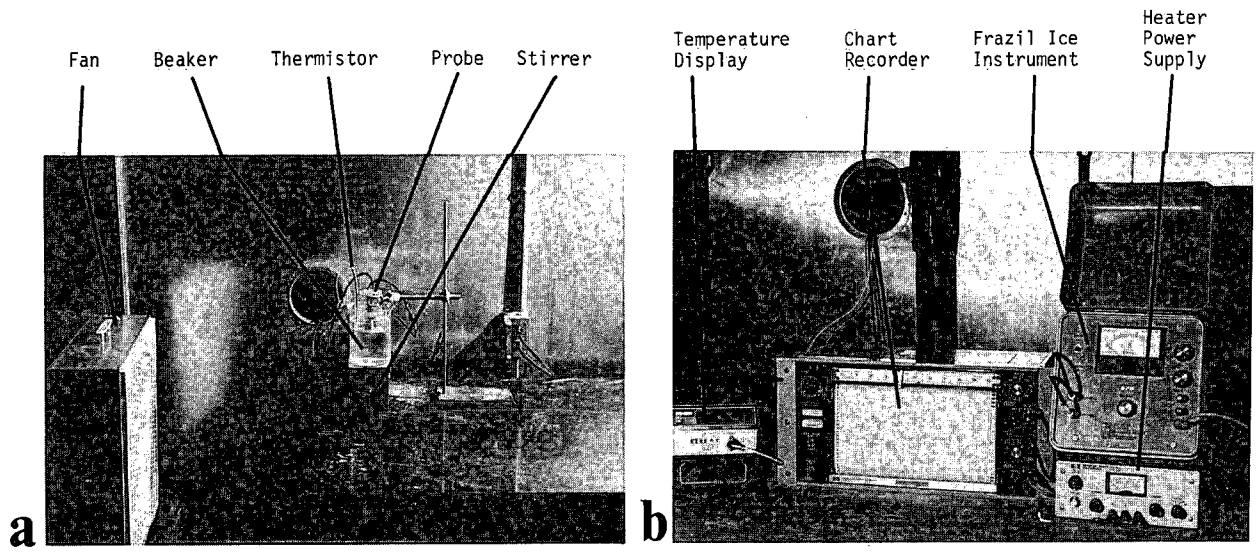

Figure 8. Experimental setup for testing the frazil ice instrument: (a) inside the cold room and (b) outside the cold room.

The generation of turbulence by a magnetic stirrer has the advantage of eliminating spraying and splashing. Thus spontaneous seeding of frazil ice produced by the falling ice particles formed in the air as a consequence of spraying and splashing of the water is avoided. The experiments showed that when only the thermometer was placed in the beaker, there was little breaking of the water surface caused by its presence and the water could be quite easily supercooled to as much as -6°C. When the experimental probe was placed in the beaker, however, there was some occasional breaking of the surface, which led to earlier spontaneous formation of frazil ice or surface ice. Generally, with the presence of the probe, it was difficult to obtain more than -1°C supercooling. The formation of ice in the experiments was initiated by seeding the supercooled water with a lump of ice. Ice was seen forming quickly as the seeding ice lump reached the magnetic bar and was broken up. Just before seeding the fan was turned off, and as soon as ice began to form, the magnetic stirrer was also turned off. Immediately after ice formation, the power input to the heaters of the probe was changed from that governed by equation (40) to that governed by equation (42).

The ice formed in the supercooled water was either in the form of needles or flakes. These two forms of dynamic ice are shown in Figure 9. The ruler in Figure 9a indicates the size of the beaker and the ice crystals. The division of these two forms of ice was approximately -1.9°C. For supercoolings above this critical temperature, needle-shaped frazil ice was formed and for supercoolings colder than this critical temperature, flake-shaped frazil ice was produced. The needle-shaped frazil ice floated and moved slowly with the water, whereas the flake-shaped ice formed a beehive-like, but much more irregular and complicated, buildup that effectively stopped the movement of the water. In the experiments testing the instrument, only needle-shaped frazil ice was formed.

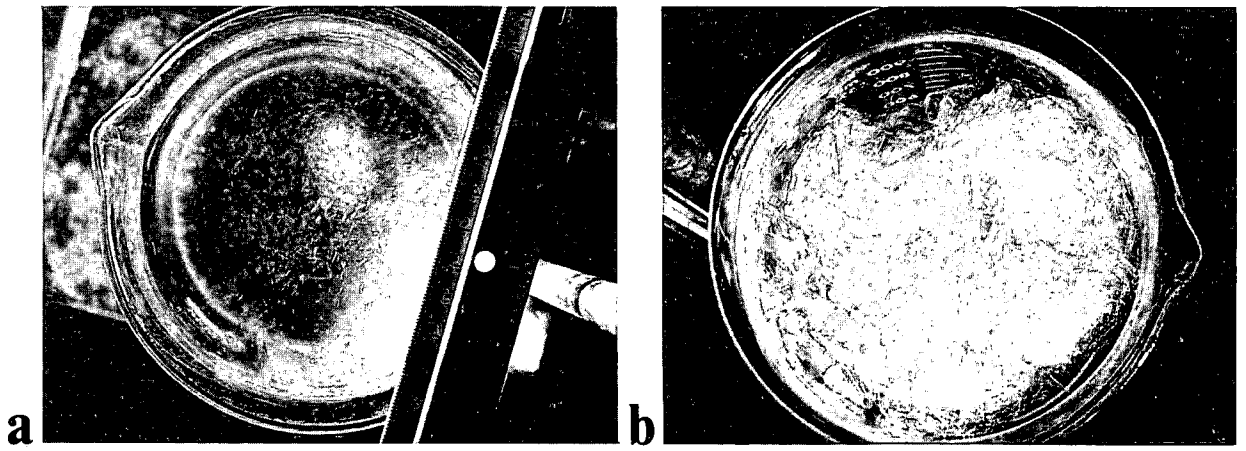

Figure 9. Two types of dynamic ice formed in the experiments: (a) needle-shaped frazil ice formed above -1.9°C and (b) flake-shaped ice crystals formed below -1.9°C.

Figure 10a is the typical output of an experimental test; it shows the simultaneous temperature and instrument output recordings. It is seen from Figure 10a that the temperature of the water decreased almost linearly under the tested conditions. The change of the cooling rate as the fan was switched from high to low is also evident. The linear temperature depression continued to the minimum point at which the frazil ice was seeded. The temperature curve indicates that as soon as ice was formed and the latent heat of fusion was released, the temperature of the water quickly rose to 0°C and maintained that temperature as ice was continuously formed.

A clear correlation between the output of the instrument and the temperature recording is shown in Figure 10a. The signal output increased rapidly following seeding, indicating growing frazil concentration in the water. The signal output increased much slower after the frazil run was finished and the water temperature reached 0°C because the rate of heat loss was reduced by switching off the fan and the stirrers. Following the frazil run, the ice formed was mainly surface ice. The slow upward drifting of the instrument signal prior to frazil formation was caused by the temperature dependence of the conductivity of water. If probe x and probe y had been exactly the same, the effect of temperature on the conductance of one probe would have compensated for the effect on the other and there would have been no upward drifting. It is interesting to note in the diagram that after 0°C was reached, the upward drifting of the signal was gone, indicating the conductivity of supercooled water was independent of temperature.

Theoretically, the temperature and the signal output curve should rise at the same time because the formation of frazil ice is accompanied by the liberation of latent heat and consequently the heating up of the water. Figure 10a, however, shows that the temperature curve began to climb several seconds before the output signal climbed. One should not be concerned by this because it was caused by the mechanical inertia of the recorder, rather than by the incapability of the instrument.

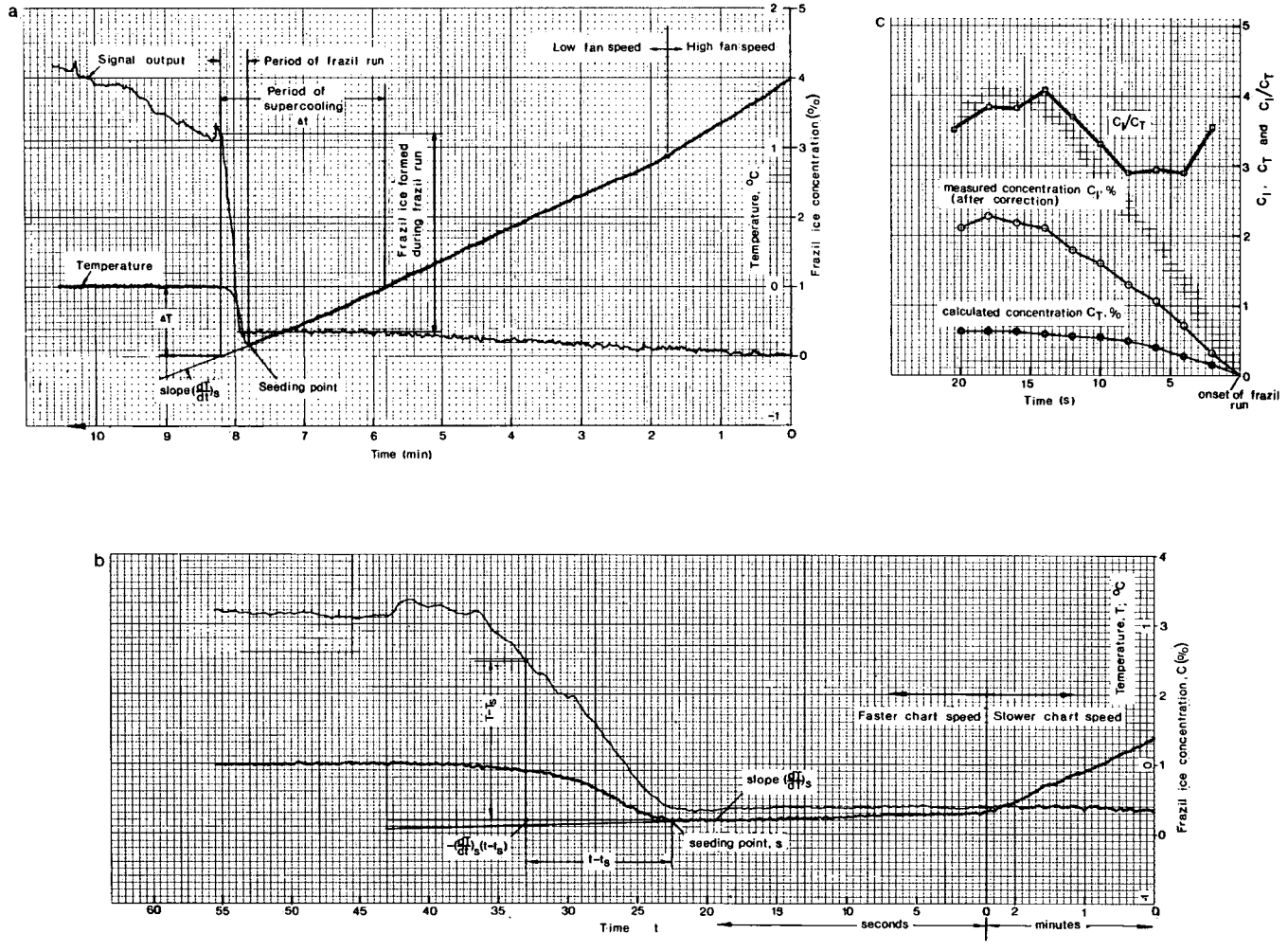

Figure 10. Typical experiment results: (a) temperature depression and instrument signal output; (b) expanded temperature and frazil ice recordings for the frazil run period; and (c) comparison of measured and calculated concentrations during the frazil run.

Figure 10b is a simultaneous recording of Figure 10a on another chart recorder at a faster speed. It is seen from Figure 10b that the signal output curve in this case climbed slightly (about 1 s) ahead of the temperature curve.

The concentration of frazil ice, as shown on Figure 10, has to be corrected to give the true experimental frazil ice concentration because the experimental condition was different from the electrical calibration condition of the instrument. Before the experiments, the instrument was electrically calibrated with a resistance of 1000 Ω substituted for R_y and a resistance of 1100 Ω substituted for R_x, and switch S_1 was connected to R_a for the 0-10% sensitivity range. Also R_3 was set under the electrical calibration condition above. It is seen from Figure 5 that under such a calibration condition when S_2 is closed, the voltage input to the amplifying circuit e_B, or the voltage at point B, is equal to half the excitation voltage to the sensing bridge.

The water used for the experiments did not give a resistance of $R_{y_0} \simeq R_y$ of 1 kΩ to the reference probe. Measurements of R_{y_0} at the University of Waterloo [80 km from Canada Centre for Inland Waters (CCIW)] showed values of R_{y_0} from 350 Ω to 425 Ω. If the mean resistance of R_{y_0} = 390 Ω is assumed for the tested water, then to give a full-range ammeter deflection when S_2 is closed, R_A in Figure 5 has to be adjusted so that the excitation voltage to the bridge will be

$$\frac{1000 + 390}{390} e_B = 3.56\, e_B$$

which is 1.78 times the excitation voltage under the electrical calibration condition. Since the bridge output under the tested condition was Δ times the excitation voltage, the frazil ice concentration reading from the instrument under the tested conditions therefore should be divided by the factor of 1.78 to give the true Δ sensed by the bridge.

It was noted later that due to calibration errors, the instrument was not electrically calibrated to give 100% full-range ammeter deflection, but to give 90% ammeter deflection. Because of these errors, the correction factor was modified from 1.78 to 1.62.

The lower resistance of the probes under tested conditions than under electrical calibration conditions affected not only the excitation voltage to the bridge but also the output of the bridge Δ. Earlier theoretical investigations show that the signal output of the sensing bridge and the concentration of frazil ice in the sensor probe are related by equation (34). Dropping the terms containing $\bar{c}$, because of its small magnitude compared with unity, reduces equation (34) to

$$\Delta = -\frac{N}{(1 + N)^2} c \qquad (43)$$

Under the electrical calibration conditions, one has N = 1, and equation (43) is reduced to

$$\Delta = -\frac{c}{4} \tag{44}$$

Under the experimental conditions, one has N = 0.39 and equation (43) becomes

$$\Delta \simeq -\frac{c}{5} \tag{45}$$

Comparison of equations (44) and (45) shows that for the same ice concentration or the same change in resistance in the sensor probe as compared with the reference probe, the signal output from the bridge under the tested conditions would be 20% less than that under the electrical calibration conditions. Thus, the concentration of frazil ice as read from the instrument should be increased by 20% to give the "true" concentration. Taking this into consideration, the earlier correction factor of 1.62 was further modified to 1.35.

From recordings similar to Figure 10, the concentrations of frazil ice at the end of the frazil ice runs were read off and corrected (Table 1).

The concentration of frazil ice may also be calculated from the temperature depression curves. It is seen from Figure 10 that theoretically the concentration of frazil ice at the end of the frazil run is given by

$$c = \frac{c_h \int_{\Delta t} -\frac{dT}{dt}\, dt}{h_L} \times 100\% \tag{46}$$

where c_h is the specific heat of water and is equal to 1 cal/g °C, dT/dt is the rate of temperature depression of the supercooling water, h_L is the latent heat of fusion and is equal to 80 cal/g, and Δt is the time period from the onset of supercooling to the end of frazil run, which is given by the point of the temperature returning to 0°C. It is seen from Figure 10a that approximately one has

$$c = \frac{-c_h \Delta T}{h_L} \times 100\% \tag{47}$$

where ΔT is obtained by projecting the temperature curve to the point of regaining 0°C. According to equation (47), the theoretical frazil ice concentration was calculated for all the tests (Table 1). Also shown in Table 1 is the ratio of the concentration of frazil ice, as detected by the instrument c_i, to the theoretical concentration of frazil ice c_t. The

Table 1. Frazil Ice Concentration Measured by the Instrument and Calculated from the Temperature Depression Curve

Test	ΔT °C	c_{int}%	c_t%	c_i%	c_i/c_t	Mean c_i/c_t
1	0.39	1.86	0.4875	1.378	2.826	3.259
2	0.44	2.28	0.55	1.689	3.071	
3	0.45	2.50	0.55625	1.852	3.329	
4	0.46	2.92	0.575	2.163	3.762	
5	0.50	2.79	0.625	2.067	3.307	
6	0.51	3.76	0.6375	2.785	4.369	3.060
7	0.51	2.05	0.6375	1.519	2.382	
8	0.60	2.46	0.75	1.822	2.430	
9	0.62	2.20	0.775	1.630	2.103	3.235
10	0.63	3.31	0.7875	2.452	3.113	
11	0.64	5.80	0.80	4.296	5.370	
12	0.65	2.80	0.8125	2.074	2.553	
13	0.65	4.32	0.8125	3.200	3.938	
14	0.66	3.75	0.825	2.778	3.367	
15	0.68	3.40	0.85	2.519	2.963	
16	0.70	2.92	0.875	2.163	2.472	
17	0.74	3.88	0.925	2.874	3.107	3.520
18	0.75	5.20	0.9375	3.852	4.109	
19	0.75	3.95	0.9375	2.926	3.121	
20	0.80	5.05	1.0000	3.741	3.741	
21	0.82	3.85	1.025	2.852	2.782	3.009
22	0.82	3.33	1.025	2.467	2.407	
23	0.84	5.94	1.05	4.400	4.190	
24	0.87	3.90	1.0875	2.889	2.656	
25	0.97	8.40	1.2125	6.222	5.132	4.480
26	1.02	5.52	1.275	4.089	3.207	
27	1.03	8.30	1.2875	6.148	4.775	
28	1.07	8.72	1.3375	6.459	4.829	
29	1.09	8.20	1.3625	6.074	4.458	
					Median = 3.31	Mean = 3.444

Note: Δt = temperature depression, see Figure 10a.

c_{int} = concentration of frazil ice as read from the instrument.

c_t = concentration of frazil ice calculated from the temperature depression curve.

c_i = instrument-read concentration of frazil ice after correction.

mean value of c_i/c_t is 3.44 and the median value is 3.31. The linear correlation that passes through the origin as the physics requires and gives a 90% confidence is approximately

$$c_i/c_t = \left(1 \pm \frac{0.52}{0.28}\right) 3.31 \tag{48}$$

This correlation was for the end of the frazil runs. Similar correlations may also be obtained for any instant within the period of frazil runs. It is seen from the temperature depression curve in Figure 10a that before the seeding of frazil ice, the water had been losing heat at a rate of $c_h\ (dT/dt)_s$, where $(dT/dt)_s$ is the negative slope of the temperature curve before seeding. This ambient heat loss of the supercooling water should remain approximately the same during the short period of frazil formation. During the period of frazil run, because of the liberation of latent heat accompanying the formation of frazil ice, the temperature of the water climbed instead of continuing to fall (Fig. 10a). From the conservation of heat for any given instant, one may thus write the following equation

$$c_h \frac{dT}{dt} = h_L \frac{dc}{dt} + c_h \left(\frac{dT}{dt}\right)_s \tag{49}$$

The integration of equation (49) gives

$$c = \frac{c_h}{h_L} \left[\left(T - T_s\right) - \left(\frac{dT}{dt}\right)_s \left(t - t_s\right)\right] \tag{50}$$

where the subscript s indicates the instant of seeding at which the concentration of frazil ice is zero. The terms within the brackets in equation (50) are readily measurable from the temperature depression curve, as shown in Figure 10b. Based on equation (50), the concentration of frazil ice for the period of frazil run in Figure 10b was calculated and is shown in Figure 10c. In Figure 10c, the concentration of frazil ice sensed by the instrument after correction is also shown. The ratio of c_i/c_t for the period of frazil run (Fig. 10c) varied between 2.90 and 4.08 with a mean value of 3.46, which is not very different from the value of 3.307 for the end of the test run (Table 1, test 5). Because of the mechanical inertia of the chart recorder, the seeding point shown on the temperature depression curve and the seeding point shown on the frazil ice concentration curve in Figure 10b (and other similar recordings) are slightly different. It was rather subjective to realign these two points while constructing Figure 10c. The above, alone, could easily give 5% to 10% difference in the value of c_i/c_t.

From the laboratory tests, one may conclude that the experimental instrument can sensitively and quantitatively detect the presence of frazil ice. An instrument based on the theoretical principles shown in the report, therefore, will have much promise.

DISCUSSIONS ON THE EXPERIMENTAL INSTRUMENT AND ITS EVALUATION

Although for individual tests the experimental instrument gave good quantitative measurements of frazil ice, the correlation between the instrument output and the calculated frazil ice concentration appeared to vary from test to test. For the tests performed, equation (48) shows that the c_i/c_t ratio could be 52% above and 28% below the median value at 90% confidence. Apparently such a highly varied correlation is not satisfactory for an instrument intended for scientific measurements.

The reason for this variation in the correlation relationship is the imperfect calibration technique. Although in the tests only the frazil ice formed inside the protective cap was sensed, in this small confined volume the distribution of frazil ice was still not uniform. It is seen from Figure 9 that the frazil ice crystals tend to cluster to give a spatial variation of their concentration. Whether the sensor probe was in the "thick" or "thin" regions could have produced a substantial difference in signal output.

This reason, however, is minor compared with the weak design of the bridge; spatial variation in concentration in the small confined volume alone should not give two measurements that are 2.5 times different under almost identically tested conditions (Table 1, tests 9 and 11). The weak design of the bridge is caused by the parallel connection of the adjustment resistances R_{xp} and R_{yp}. It is seen from Figures 5 and 6 that the equivalent resistances on the x and y arms of the bridge are, respectively,

$$R_{ex} = \frac{R_x R_{xp}}{R_x + R_{xp}} \qquad \text{and} \qquad R_{ey} = \frac{R_y R_{yp}}{R_y + R_{yp}} \tag{51}$$

When the bridge is balanced, one has $R_{ex} = R_{ey}$ or

$$\frac{R_x R_{xp}}{R_x + R_{xp}} = \frac{R_y R_{yp}}{R_y + R_{yp}} \tag{52}$$

From Figure 5, one also sees that

$$R_{yp} = R_p - R_{xp} \tag{53}$$

The substitution of equation (53) into equation (52) and its expansion lead to

$$\left(1 - \frac{R_y}{R_x}\right)\left(\frac{R_{xp}}{R_p}\right)^2 + \left(\frac{R_y}{R_x} - 2\frac{R_y}{R_p} - 1\right)\frac{R_{xp}}{R_p} + \frac{R_y}{R_p} = 0 \tag{54}$$

Since in the instrument design R_p is much greater than R_y, one has

$$\frac{R_y}{R_p} \rightarrow 0 \tag{55}$$

The application of the condition above to equation (54) leads to

$$\frac{R_{xp}}{R_p} \rightarrow 1 \qquad \text{or} \qquad R_{xp} \rightarrow R_p \tag{56}$$

Since the bridge is symmetric, one also has

$$R_{yp} \rightarrow R_p \tag{57}$$

The simultaneous existence of equations (56) and (57) means the balance of the bridge is not sensitive to the potentiometer R_p. A small variation in R_x relative to R_y can cause a wide change in R_{yp} (or R_{xp}) for the bridge to regain balance. This was indeed observed, since it was noticed during the experiments that the knob controlling R_p had to be adjusted over quite a wide range to compensate for the small changes in the resistance between the probe plates as a consequence of the daily variations of the resistivity of the tap water, the accidental bangings of the probe, and the accumulations of grease and dirt on the surface of the plates.

The sensitivity of R_{xp} and R_{yp} to changes in R_x and R_y caused the instrument to give different signal outputs for the same frazil ice concentration. It is seen from Figure 5 that the instrument measures the changes in R_{ex}; R_{ex} is given by the first equation of equation (51). The differentiation of that equation with respect to frazil ice concentration c gives

$$\frac{dR_{ex}}{dc} = \frac{1}{(1 + R_x/R_{xp})^2} \frac{dR_x}{dc} \tag{58}$$

Equation (58) shows that the change in R_{ex} not only depends on the change in R_x alone but also on the ratio R_x/R_{xp}. Since R_{xp} is capable of wide variation while R_x changes little, the correlation between the signal output and the frazil ice concentration therefore can be highly different from test to test.

Understanding the above, the instrument can be made to give a better signal-output frazil-concentration correlation by using variable resistances connected in series with R_x and R_y for fine adjustment of the bridge instead of the present design.

The high value of the median of the measured concentration to calculated concentration ratio of 3.31 presents a pleasing, but unexplainable, puzzle at this point. Although the small resistivity of the tested water created a corrective factor of 1.35 for the present tests, it can be shown that the corrective factor can at the most reach a value of 1.8 and that happens when the resistivity of the tested water becomes negligible. With a corrective factor of 1.8, the median value of c_i/c_t of 3.31 is modified to 2.48, which is still a high value.

The shape and the finite size of the ice crystals may be the other factors responsible for the magnified effect of frazil ice on the resistance of the tested water. By considering a frazil ice crystal as approximately an elongated spheroid with a length to breadth ratio of 10:1, the Appendix shows that the resistance effect based on fractional displacement theory should be increased by a multiplying factor of 1.65. Nevertheless, even with this factor taken into account, the median value of c_i/c_t would still be 2.0. Further theoretical investigation of the causes of the high c_i/c_t ratio is beyond the scope of this report. The magnified effect of frazil ice on water resistance, however, is beneficial because it will make the instrument more sensitive and the hardware design will be easier.

The equation relating the signal output of the sensing resistance bridge and the concentration of frazil ice, equation (34), may be rewritten as

$$\Delta = \frac{-N_*}{(1 + N_*)^2} c \tag{59}$$

where $$N_* = \frac{R_y}{R_1} \tag{60}$$

Because the values of N_* were different between calibration and the test conditions, the measured concentrations had to be corrected for the experimental instrument. To eliminate the necessity of measuring the resistance of the ice-free water between the probe plates (R_y) and the correction process, the instrument should be designed so that N_* is a constant, preferably equal to unity.

The circuitry that gives $N_* = 1$ is shown in Figure 11. Figure 11a is made up of three resistance bridges which demonstrate how $N_* = 1$ is obtained step by step. The first bridge is for adjusting R_1 to be equal to R_y. After $R_1 = R_y$ is obtained, the substitution of R_y by R_2, as shown by the second bridge and the subsequent adjustment, gives $R_1 = R_2 = R_y$. The use of $R_1 = R_2 = R_y$ in the third bridge gives the sensing bridge of the instrument with $N_* = 1$. Figure 11b is the circuit that comprises the three bridges. By switching the switches to positions 1, 2 and 3, as indicated, the three bridges shown in Figure 11a will be formed. The design shown on Figure 11 has the advantage that it enables the calibration (or zeroing) of the instrument under working conditions.

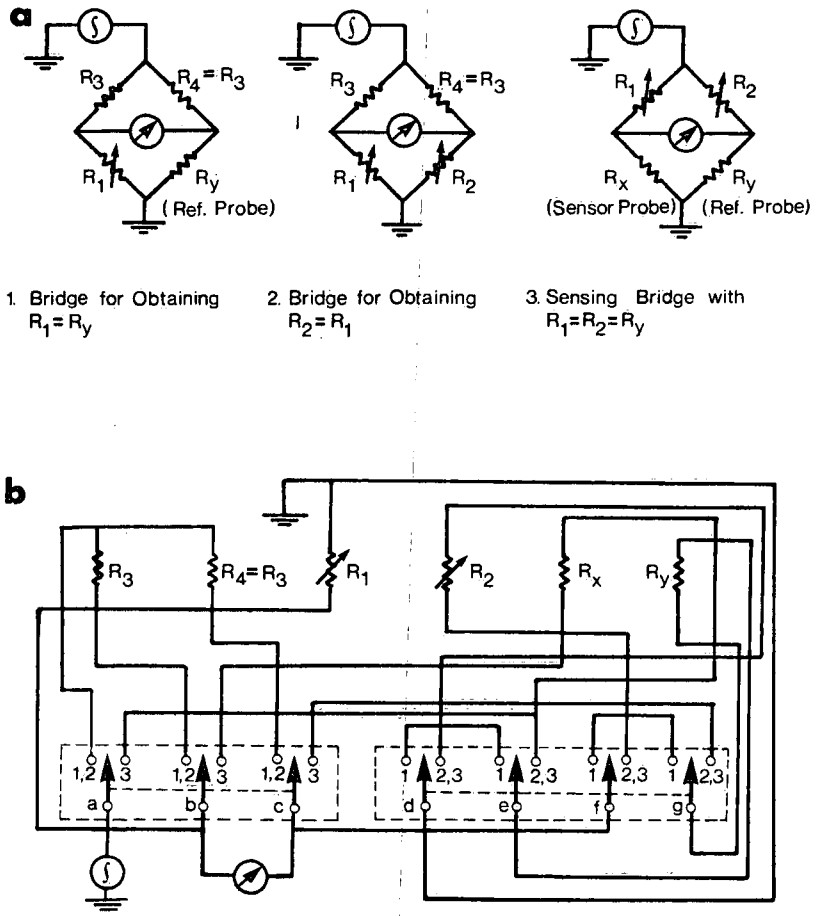

Figure 11. Circuit for obtaining $N_* = 1$: (a) bridge arrangements for obtaining $N_* = 1$ and (b) circuitry comprising the three bridges in (a).

The experimental probe described here is far from satisfactory. Since the probe plates were rectangular, it was hard to make them identical. The outside of the side plates was exposed to the ambient fluid, and the stray of the electric lines from the edges and corners was excessive. In addition, the probe was unnecessarily bulky and structurally weak. Therefore the probe must be redesigned.

To measure frazil ice under different conditions, different probes are needed. Figure 12 shows the conceptual design of two probes. The probe in Figure 12a is for measuring frazil ice in waters where turbulence is mainly induced by surface waves or agitation. The probe in Figure 12b is for frazil ice sensing when a noticeable mean flow is present. It is recommended that in phase II of the instrument development, probes should be constructed according to Figure 12.

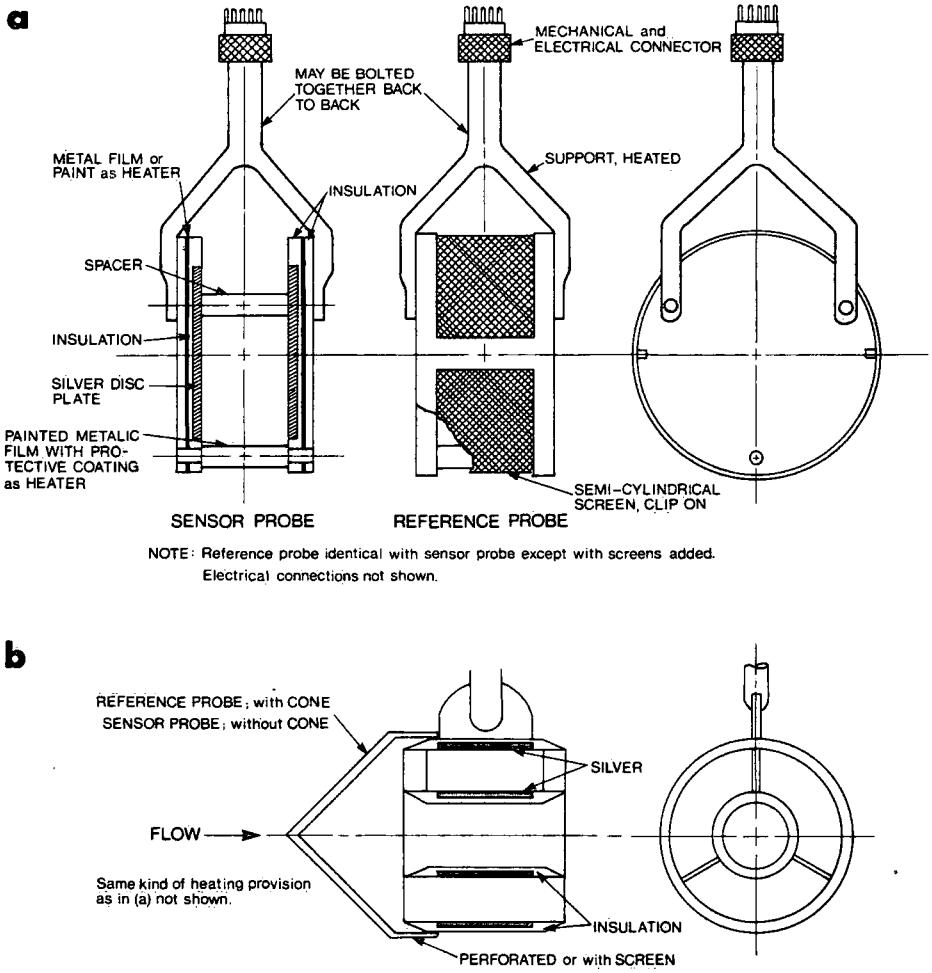

Figure 12. Conceptual design of improved probes showing (a) a probe for water with low mean velocities and (b) a probe for flowing water.

Although it has been shown that theoretically an instrument built on the capacitance sensing principle has the advantage of having M = 1, or that the measurement is not affected by the source of water, there are problems in the hardware design of such an instrument. These problems occur because of the small capacitance involved. For scientific usage of the instrument, it is desirable that the sampled volume is approximately cubic. In such a situation the area to separation ratio of the probe plates A/S is approximately equal to S. The substitution of this value of A/S into equation (10) with $\varepsilon_{H_2O} = 80 \times \frac{1}{36\pi} \times 10^{-9}$ F/m indicates the capacitance of the reference probe to be $C_y \simeq S \times 10^{-9}$ F. Even with a huge plate separation of S = 1 m the capacitance that one has to handle is still only 10^{-9} F, which is a very small capacitance. Building a capacitance instrument thus becomes a problem of technological feasibility.

CONCLUSIONS

At the conclusion of phase I of the instrument development, it may be said that scientifically the quantitative measurement of frazil ice concentration is possible by sensing the effect of frazil ice on the resistivity or on the dielectric constant of water. Theoretical investigations show that a capacitance instrument appears to have a certain advantage over a resistance instrument. The construction of a capacitance instrument, however, is constrained by the small capacitance involved that one must successfully handle. The problem thus becomes technological. An experimental instrument based on the resistance principle has been built and tested. The experimental instrument shows much promise. Further development of the instrument should produce a manufacturable prototype.

The effect of frazil ice on the resistivity of water needs more investigation. Yet this does not affect the development of the instrument if an instrument is to be calibrated before it is used. The unexpected high sensitivity of the resistance of water with ice present is beneficial because it increases the sensitivity of the instrument.

Because of the clustering of frazil ice crystals, the calibration of an instrument will always be a problem. A better calibration technique than the one described here will be very desirable.

ACKNOWLEDGMENTS

Mr. Kenneth Hill, a member of the ice research group of the Hydraulics Section, has been involved in most of the laboratory testing of the instrument, and Mr. Charles Der, an electronic engineer from the Engineering Support Section, has helped in electronic technological matters. Their diligent work is gratefully acknowledged.

REFERENCES

Gilfilian, R.E., W.L. Line and T. Osterkamp. 1972. Ice formation in a small Alaskan stream, UNESCO-5: Properties and process of river and lake ice. University of Alaska.

Kristinsson, B. September 1970. Ice monitoring equipment. *Proceedings* IAHR Symposium on Ice and its Action on Hydraulic Structures, Reykjavik, pp. 1.1, 1-14.

Schmidt, C.C., and J.R. Glover. 1975. A frazil ice concentration measuring system using a laser doppler velocimeter. *J. Hydraul. Res.*, IAHR, Vol. 13, No. 3, pp. 299-314.

Tsang, G. 1974. Conceptual design of a multi-purpose instrument for winter stream metering. *Proceedings* International Symposium on Advanced Concepts and Techniques in the Study of Snow and Ice Resources, Monterey, December 1973, pp. 688-698. Published by the United States National Academy of Sciences.

APPENDIX *

In the theoretical development part of the report, the fractional displacement theory was used that the presence of frazil ice reduces proportionally the number of ions in the volume between the probe plates and the conductive area of the plates, and from this theory equation (8)

$$\frac{R_x}{R_y} = \frac{1}{1 - c} = 1 + c \tag{A.1}$$

and equation (21)

$$\rho_0 = (1 - \bar{c})\, \rho_{H_2O} \tag{A.2}$$

were obtained. The extension of the fractional displacement theory to the dielectric constant of the medium gave equation (11)

$$\varepsilon_x = (1 - c)\, \varepsilon_{H_2O} + c\, \varepsilon_{ice} \tag{A.3}$$

Equations (A.1) and (A.2) are only true under two specific conditions. The first is that the ice particles are so small that they do not affect the electric line between the plates, and the second is that the ice forms long rods extending from one plate to the other and in so doing proportionally reduces the conductive area of the plates. Equation (A.3) is only true under the second condition. For frazil ice, since the ice crystals are finite in size and distributed randomly in space, both in quantity and orientation, neither of the conditions above are satisfied and equations (A.1) to (A.3) thus are not valid. This probably is one of the reasons for the larger measured values of frazil ice concentration than the theoretically predicted values.

For better mathematical expressions for later comparisons, conductivity τ will be used in place of resistivity. With the fractional displacement theory, the change in conductivity of the medium following the formation of frazil ice is given by

$$\Delta\tau = - c\tau \tag{A.4}$$

Because the presence of the randomly distributed and oriented frazil ice crystals causes the diversion of the electric lines, the reduction in conductivity will be more than that

*Professor Y.L. Chow, Department of Electrical Engineering, University of Waterloo, has been consulted on the work presented in the Appendix.

shown by equation (A.4) and to account for this, a multiplying factor m_τ greater than unity may be used to change equation (A.4) to

$$\Delta\tau = - m_\tau c\tau \tag{A.5}$$

Equation (A.3) gives the dielectric constant of the frazil ice-laden water. The change in dielectric constant from the ice-free condition to the ice-laden condition may be obtained from it to be

$$\Delta\varepsilon = - \varepsilon_{H_2O} (1 - \gamma_\varepsilon) c \tag{A.6}$$

where $\gamma_\varepsilon = \varepsilon_{ice}/\varepsilon_{H_2O}$, as has been defined earlier in the text. Similar to the conductivity case, another multiplying factor m_ε may be introduced to take into account the diversion of the dielectric field line and equation (A.6) becomes

$$\Delta\varepsilon = - m_\varepsilon \varepsilon_{H_2O} (1 - \gamma_\varepsilon) c \tag{A.7}$$

It may be pointed out that m_τ and m_ε are different because although physically frazil ice may be considered as an insulator through which the electric lines cannot penetrate, it may not be considered as impermeable to dielectric field lines because it has a finite, although small, relative dielectric constant (5/80) with respect to water.

To evaluate m_ε, the polarization theory may be used. According to the theory, for water with suspended frazil ice particles, the polarization induced by an electric field $\vec{E}$ is given by

$$\vec{P} = n\alpha \varepsilon_{H_2O} \vec{E} \tag{A.8}$$

where n is the number of ice crystals per unit volume and α is the polarizability of an ice particle. In equation (A.8), $\vec{E}$ is the field including the applied field and the field from the dipoles produced by the applied field. For low ice concentrations, which generally are the case, $\vec{E}$ may be considered as approximately equal to the applied field.

From the definition of displacement flux density, one sees that the displacement flux density between the probe plates is given by

$$\vec{D} = \varepsilon_{H_2O} \vec{E} + \vec{P} = \varepsilon_{H_2O} (1 + n\alpha) \vec{E} \tag{A.9}$$

By definition one also has

$$\vec{D} = \varepsilon_{med} \vec{E} \tag{A.10}$$

where ε_{med} is the dielectric constant of the water and frazil ice mixture. From the two equations above, one has

$$\Delta\varepsilon = \varepsilon_{med} - \varepsilon_{H_2O} = \varepsilon_{H_2O}\, n\alpha \tag{A.11}$$

which is the change in dielectric constant as the water between the probe plates changes from ice-free to ice-laden. From equations (A.7) and (A.11) one has

$$m_\varepsilon = -\frac{n\alpha}{(1-\gamma_\varepsilon)\, c} = -\frac{\alpha}{(1-\gamma_\varepsilon) V_p} \tag{A.12}$$

where $V_p = c/n$ is the volume of an (average) ice crystal.

The polarizability, or electric susceptibility α of an ice crystal, is a function of its orientation and shape and the dielectric constant ratio γ_ε. If frazil ice crystals can be considered as ellipsoidal particles (in fact, frazil ice crystals are in needle form as shown in Figure 9), Stratton (1941) showed that when the electric field is parallel to one of its principal axes, the polarizability is given by

$$\alpha_i = \frac{V_P}{L_i + \dfrac{1}{(\gamma_\varepsilon - 1)}} \tag{A.13}$$

where the subscript i indicates one of the principal axes, and L_i is given by

$$L_i = \frac{\ell_1 \ell_2 \ell_3}{2} \int_0^\infty (s + \ell_i^2)^{-1} \left[(s+\ell_1^2)(s+\ell_2^2)(s+\ell_3^2)\right]^{\frac{1}{2}} ds \tag{A.14}$$

where ℓ_1, ℓ_2 and ℓ_3 are the three dimensions along the principal axes. Since the orientation of the frazil ice crystals is random, one may simplify the matter by considering that one third of all the crystals has its first principal axis, another third has its second principal axis, and the last third has its third principal axis aligned with the applied electric field. With such a simplification, the average polarizability of the ice crystals in mass is given by

$$\alpha = \frac{\alpha_1 + \alpha_2 + \alpha_3}{3} \tag{A.15}$$

With equations (A.12) to (A.15), the multiplying factor m_ε is calculated for a few spheroid cases (Table A-1).

Table A-1. Multiplying Factors m_ε and m_τ for Some Spheroids

Case	ℓ_1	ℓ_2	ℓ_3	m_ε	m_τ
Sphere	1	1	1	1.45	1.50
Prolate spheroid	10	1	1	1.57	1.65
Very long spheroid	∞	1	1	1.59	1.67
Oblate spheroid	1	5	5	1.88	2.09
Flat spheroid	1	10	10	2.44	3.02
Thin disc	1	∞	∞	6.00	∞

Note: (1) The volume of the spheroid is immaterial because V_p disappears from the final relationship by cancelling.

(2) The electric field is in the ℓ_1 direction.

The multiplying factor m_τ for conductivity may also be obtained by a similar method from equation (A.5) and the definition equation for conductivity

$$\vec{J} = \tau \vec{E} \tag{A.16}$$

where $\vec{J}$ is the current density. A comparison of equation (A.16) and equation (A.10), however, shows that these two equations are identical. Thus any solution obtained for dielectric constant can be directly applied to conductivity. A comparison of equations (A.5) and (A.6) indicates that if $\gamma_\varepsilon = 0$, the two equations will be of exactly the same form. Thus, according to the above, by assigning $\gamma_\varepsilon = 0$, the multiplying factor m_τ may also be calculated from equations (A.12) to (A.15). The calculated values of m_τ for different spheroid cases are also shown on Table A-1.

Table A-1 shows that m_ε and m_τ have the least value for a sphere. The elongation and the compression of the sphere both increase the values of m_ε and m_τ. It is seen from Figure 9 that frazil ice crystals may be considered as approximately prolate spheroids with dimensions $\ell_1 : \ell_2 : \ell_3 = 10:1:1$ and thus give a conductivity multiplying factor of $m_\tau = 1.65$.

The use of this multiplying factor in the experimental results changes the median value of the c_i/c_t ratio from 3.31 to 2.00. The measured frazil ice concentration is still twice the calculated concentration.

REFERENCE

Stratton, J.A. 1941. *Electromagnetic Theory*. McGraw-Hill.